Effect of Alkali Metal Cations on the Structure of Mo(VI)/SiO$_2$ Catalysts and Its Relevance to the Selective Oxidation of Methane and Methanol

Miguel A. Bañares, Nicholas D. Spencer,[*][1] Michael D. Jones,[*] and Israel E. Wachs

*Zettlemoyer Center for Surface Studies, Lehigh University, Bethlehem, Pennsylvania 18015; and *W.R. Grace & Co.–Conn., Columbia, Maryland 21044*

The effect of alkali metal additives on both the structure of MoO$_3$/SiO$_2$ and its behavior as a catalyst for selective oxidation of methane and methanol to formaldehyde was investigated. The structure of the silica-supported molybdenum oxide catalysts was determined by *in situ* Raman spectroscopy and the amount of reducible oxygen in the catalyst was determined by temperature-programmed reduction. In the absence of alkali metal, only an isolated surface molybdenum oxide species was present on the silica support. Addition of alkali metals decreased the number of isolated surface molybdenum oxide species and formed new alkali–molybdate compounds due to the weak interaction of the Mo species with the silica surface. The oxygen associated with the alkali–molybdate compounds was generally not available for oxidation reactions. Consequently, the addition of alkali metal decreased the catalytic activity for the oxidation of both methane and methanol. The activity for methane oxidation was found to correlate with the number of remaining isolated Mo species and the activity for methanol oxidation was found to correlate with the amount of reducible oxygen present in the catalyst. © 1994 Academic Press, Inc.

1. INTRODUCTION

Silica-supported molybdenum oxide catalysts have recently generated much interest due to their possible application in converting the large reserves of natural gas into more valuable products (1–7). The structures of supported molybdenum oxides seem to be decisive in their catalytic performance, and the molybdenum oxide loading is a critical factor affecting both structure and activity (7, 8). Under ambient conditions and below monolayer coverage, the molybdenum is present as a silica-supported hydrated surface polymolybdate species (Mo$_7$O$_{24}^{6-}$) whose structure depends on the surface pH at the PZC of the catalyst (8, 9). Upon dehydration, the polymolybdate structures are

unstable and spread over the silica surface to form isolated surface molybdenum oxide species possessing one terminal Mo = O bond and 5–6-fold oxygen coordination (9). Crystalline molybdenum oxide (MoO$_3$) is the dominant species at higher loadings and is stable upon dehydration. The nature and reactivity of the supported metal oxides is also affected by the presence of impurities. It has been shown that calcium impurities lead to the formation of calcium molybdate (CaMoO$_4$) at the expense of surface molybdenum oxide species (8) and that the presence of alkali metal impurities has a negative effect on the conversion of methane to formaldehyde (10). A kinetic model has been proposed to account for the poisoning of Mo(VI)/SiO$_2$ catalysts by sodium (11). A model was also proposed (11) to account for the effect of sodium on the structure of the supported crystalline molybdenum oxide. The model tried to account for the dramatic effect of very small amounts of sodium on the selective conversion of methane to formaldehyde on silica-supported molybdenum oxide catalysts.

In the present work, the sodium-doped silica-supported molybdenum oxide catalysts previously studied by one of the authors (11), as well as the corresponding potassium and cesium-doped promoted catalysts, are characterized by Raman spectroscopy, TPR and methanol oxidation. Methane oxidation was also performed on the K- and Cs-doped samples. The current findings show that there is no crystalline molybdenum oxide and provide further insight into the nature of the effect of alkali metals on the structure and reactivity of silica-supported molybdenum oxide catalysts.

2. EXPERIMENTAL

The *preparation* of the sodium-promoted molybdenum oxide on silica catalysts has been described elsewhere (11). The preparation of the K- and Cs-promoted samples follows the same procedures and incorporating amounts

of the alkali cation equivalent, on a molar basis, to the 1477 ppm Na/2.4%MoO$_3$/SiO$_2$ catalyst.

The *Raman spectra* were recorded on both hydrated and dehydrated catalysts according to the conditions previously reported (8). The *in situ* Raman spectra during methane oxidation were recorded in a Raman cell that allows running experiments in flowing gases at high temperatures. The catalyst is employed as a self-supported wafer and its temperature is controlled by a thermocouple. The reaction was carried out at 823 K in a reaction mixture comprising He : CH$_4$: O$_2$ = 50 : 10 : 10 ml/min, and the flows were controlled by needle valves and flowmeters.

The selective oxidation of methane was run as described in Ref. (12). The equipment used for the methanol oxidation experiments is described in Ref. (13). The catalytic activity results are presented as turnover frequencies (T.O.F.), expressed as the number of moles of reacted reactant or formed product per molybdena unit per second and assumes that all the molybdena is active.

Temperature-programmed reduction experiments were carried out using 400 mg of sample which were pretreated *in situ* at 673 K for 1 hour in dry air. Following pretreatment, the samples were cooled to 573 K and the gas switched to 4.99% hydrogen in argon (Matheson, primary standard). The gas flow was 50 sccm. After several minutes, during which the system became purged with the reduction gas, the temperature was raised at 20°C/min to 1273 K. During this time the exit gas was monitored using a thermal conductivity detector. The detector had previously been calibrated with both pure argon and the H$_2$/Ar reduction gas.

3. RESULTS

3.1. Raman Spectra

The Raman spectra of the different hydrated sodium-doped samples are shown in Fig. 1. The features at 480, 600, and 800 cm^{-1} are characteristic of the silica support. The sodium-free MoO$_3$/SiO$_2$ sample possesses Raman bands characteristic of ammonium heptamolybdate ((NH$_4$)$_6$Mo$_7$O$_{24}$), at 965–944, 880, 380–370, and 240–210 cm^{-1} (8, 9). The addition of sodium results in the appearance of new Raman features at 890 and 830 cm^{-1}, revealing the formation of new molybdate compounds. The presence of other alkali metal (K and Cs) also results in the appearance of new features at ca. 880 and 830 cm^{-1} which are less evident for the cesium-doped sample, as can be seen in the Raman spectra of the hydrated samples of Fig. 2.

The Raman spectra of the dehydrated sodium-doped catalysts are shown in Fig. 3 for several different Na loadings (wppm). All the samples show a band of ca. 986 cm^{-1} which corresponds to the stretching mode of the terminal bond Mo = O (14) of the dehydrated monomeric
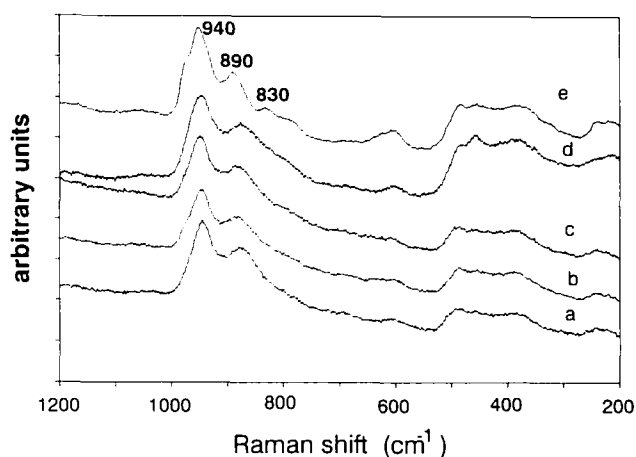

FIG. 1. Raman spectra of the hydrated sodium-free and sodium-doped samples: (a) 10 wppm Na, sodium "free"; (b) 319 wppm Na; (c) 700 wppm Na; (d) 900 wppm Na; and (e) 1447 wppm Na.

surface molybdenum oxide species on the silica support. At higher sodium loadings the samples also show new features at ca. 940, 890, and 830 cm^{-1}. The Raman band at 940 cm^{-1} was overshadowed by the heptamolybdate Raman band in the hydrated samples. These new bands are unaffected by dehydration and resemble those of sodium dimolybdate (Na$_2$Mo$_2$O$_7$) at 950, 880, and 840 cm^{-1} (15).

The Raman spectra of the other dehydrated alkali-metal-doped samples also exhibit new features that are not affected by the hydration (940, 880, and 840 cm^{-1} for the potassium-doped sample, and at ~950, 890, and 830 cm^{-1} for the cesium-doped sample), revealing the formation of new compounds similar to K$_2$Mo$_2$O$_7$ (930, 905, 873, and 860 cm^{-1}) (15) and, probably, Cs$_2$Mo$_2$O$_7$ (No
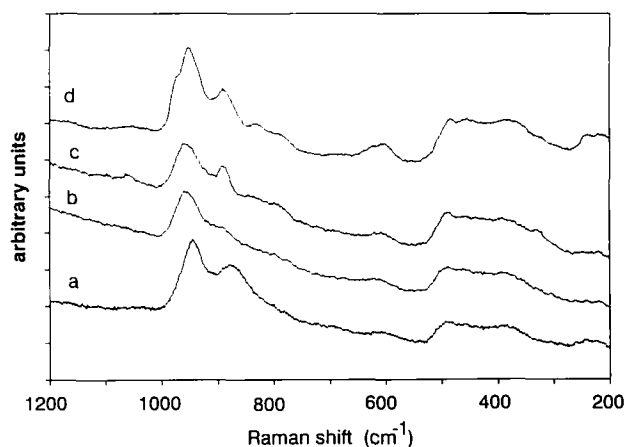

FIG. 2. Raman spectra of the hydrated alkali-doped 2.4% MoO$_3$/SiO$_2$ samples: (a) Mo : Na = 300 : 1, alkali "free"; (b) Mo : Cs = 3 : 1; (c) Mo : K = 3 : 1; and (d) Mo : Na = 3 : 1.
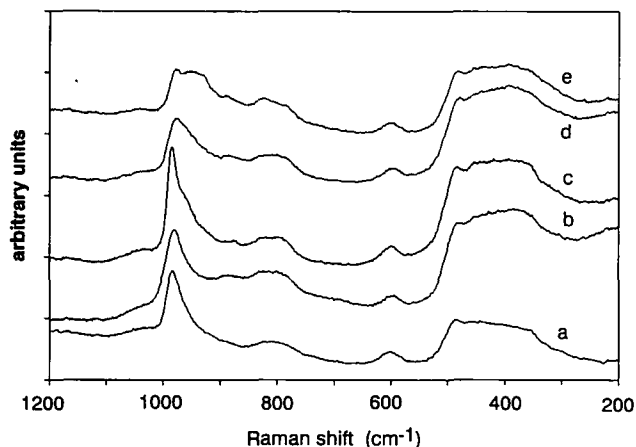
FIG. 3. Raman spectra of the dehydrated sodium-free and sodium-doped samples. (a) 10 wppm Na, sodium "free"; (b) 319 wppm Na; (c) 700 wppm Na; (d) 900 wppm Na; and (e) 1477 wppm Na.

reference was found for $Cs_2Mo_2O_7$) on silica resulting from the interaction of the alkali additives with the surface molybdenum oxide (Fig. 4).

Figure 5 shows the *in situ* Raman spectra of an alkali-free MoO_3/SiO_2 catalyst during (a) the oxidation of methane at 823 K, (b) dehydrated in flowing oxygen at the same temperature, and (c) dehydrated at room temperature. All the spectra possess the same Raman band at ca. 986 cm^{-1} which suggests that the same dehydrated surface molybdenum oxide species is present on silica under all these conditions. Consequently, the structural information from Raman spectra of the room-temperature dehydrated catalysts can be directly related to the catalytic activity in the selective oxidation of methane. A similar situation is also applicable for Mo/SiO_2 catalysts during methanol oxidation (H. Hu and I. E. Wachs, to be published).
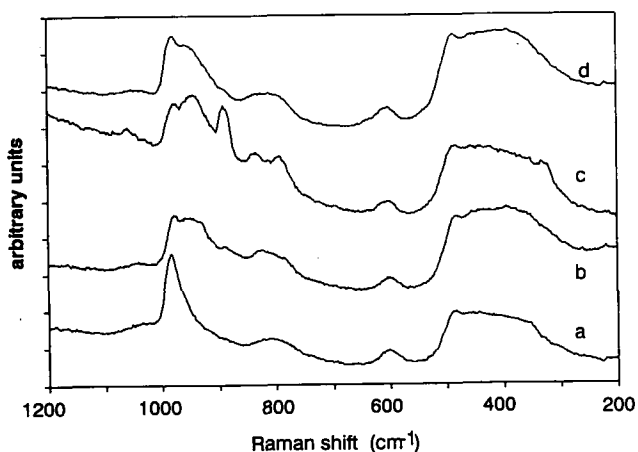
3.2. Catalytic Activity

Methane oxidation. The selective oxidation of methane mainly results in the formation of formaldehyde, CO_x, and water. Minor amounts of H_2 and CH_3OH were also detected. The turnover frequencies (T.O.F.) to the principal products are presented in Fig. 6a as a function of Na content. A decrease in the oxidation activity is observed upon the addition of sodium. According to the mechanism proposed for the reaction (1), supported by isotopic studies (16–18), HCHO and CO_2 are directly produced from methane, and CO is generated by the further oxidation of formaldehyde.

Methanol oxidation. The selective oxidation of methanol leads to the formation of formaldehyde, methyl formate, dimethyl ether and minor amounts of carbon oxides (see Fig. 6b). The incorporation of sodium into the molybdena/silica catalyst initially decreases the activity to approximately half, but additional sodium does not seem to significantly modify the activity of the catalysts.

3.3. TPR

The TPR experiments reveal that the new molybdate compounds formed upon addition of alkali are generally less reducible than the dispersed surface molybdenum oxide species on silica (with the exception of the cesium doped system). The amount of H_2 consumed is presented in Table 1. For the alkali metal doped samples, the trend in H_2 consumption is Cs > Na > K. This trend corresponds with the degree of crystallinity of the new compounds since the Raman spectra of the K-doped sample shows the sharpest bands in the series and the Cs-doped samples possesses the smoothest Raman
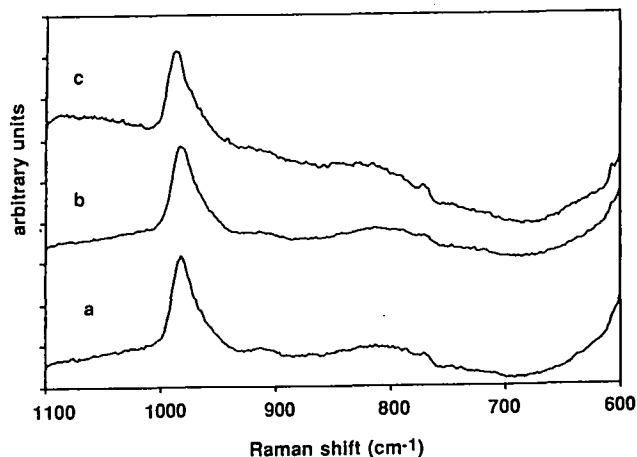

FIG. 4. Raman spectra of the dehydrated alkali metal doped 2.4% MoO_3/SiO_2 samples: (a) Mo : Na = 300 : 1, alkali "free"; (b) Mo : Cs = 3 : 1; (c) Mo : K = 3 : 1; and (d) Mo : Na = 3 : 1.

FIG. 5. *In situ* laser Raman spectra during (a) methane oxidation at 823 K, (b) dehydrated in flowing O_2 at 823 K, and (c) dehydrated in flowing O_2 at room temperature.
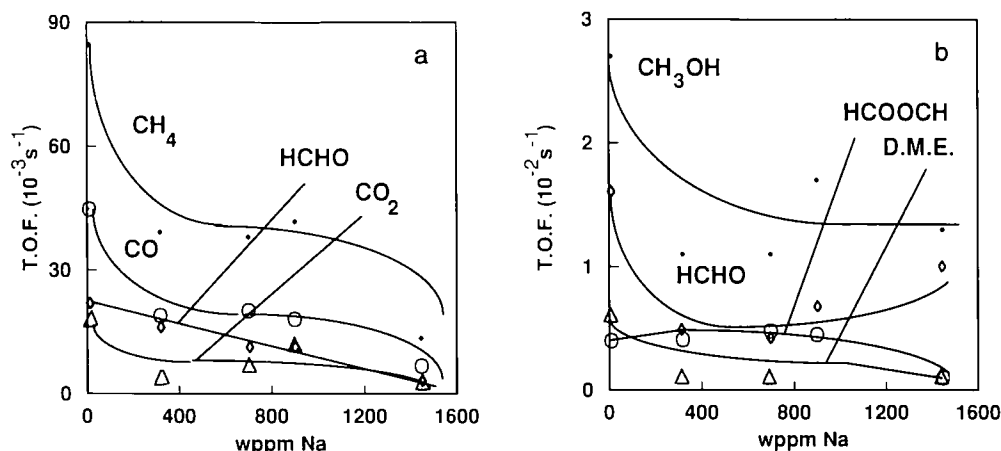
FIG. 6. (a) T.O.F. in methane oxidation at 923 K, $CH_4 : O_2$ = 9 : 1 m, GHSV(CH_4) = 5000 s^{-1}. (b) T.O.F. in methanol oxidation at 503 K.

features. The increase in hydrogen consumption for the Cs-doped sample with respect the alkali-free one is not clear at present.

4. DISCUSSION

4.1. Surface Molybdenum Oxide Species

Previous studies (9, 10) have shown that the surface molybdenum oxide species on silica, under ambient conditions, is present as hydrated heptamolybdate ($Mo_7 O_{24}^{6-}$) clusters. Upon dehydration, these species become unstable and spread on the silica surface as isolated, mono-oxo hexacoordinated surface molybdenum oxide species. Crystalline MoO_3 is formed if the molybdenum loading is above the threshold value. The crystalline MoO_3 structure is not affected by hydration–dehydration and does not disperse under dehydrated conditions on SiO_2.

The presence of other oxides can modify the structure of the supported molybdenum oxide phase. When molyb-

denum oxide is supported on silica in the presence of other acidic metal oxides (V_2O_5 or W_2O_3) there appears to be no interaction between the oxides and each behaves independently of each other (19). However, the presence of basic oxides leads to the formation of molybdenum oxide compounds (20, 22) and has been previously observed with the presence of calcium impurities in molybdena-silica catalysts (8). The new alkali–molybdate compounds formed appear to be thermally stable and not affected by hydration–dehydration treatments.

Several studies have shown that the metal oxide–support interaction is weaker with silica than with other supports such as alumina, titania, magnesia, etc. (23). Such a weak interaction is reflected by the lack of spreading of crystalline MoO_3 in physical mixtures of MoO_3 and silica upon calcination (21). On other oxide supports (Al_2O_3, TiO_2, etc.), this spreading takes place readily (21, 23). The very low maximum surface coverages achieved on silica, an order of magnitude lower than on other sup-

TABLE 1

Effect of the Alkali Metal Cations on Catalytic Activity and H_2 Consumption in TPR

Alkali additive[a]	T.O.F. (10^{-3} s^{-1})								TPR H_2 consumption (μmol H_2/g)
	CH_4 oxidation[b]				CH_3OH oxidation[c]				
	CH_4	HCHO	CO_2	CO	CH_3OH	HCHO	CH_3OCH_3	$HCOOCH_3$	
None	51.6	13.4	10.8	27.7	27.0	16.0	6.0	4.0	890
Na	14.2	3.9	3.1	7.2	13.0	10.0	1.0	1.0	730
K	50.2	7.2	16.9	26.1	3.0	2.1	0.2	0.7	490
Cs	33.3	11.7	9.4	23.9	8.0	5.0	2.0	0.1	980

[a] Atomic ratio additive : Mo = 1 : 3.
[b] Reaction conditions : 923 K; $CH_4 : O_2$ = 9 : 1 m; GHSV (CH_4) = 5000 s^{-1}.
[c] Reaction conditions: 503 K (0.01728 mol CH_3OH/h in 50 mg catalyst).

ports (24) is also significant. This weaker interaction with the silica support results in a higher degree of mobility of the surface molybdenum oxide species. Consequently, at intermediate surface coverages on silica the surface metal oxide will tend to aggregate into crystalline metal oxide phases. Thus, for silica-supported metal oxide systems this dispersion limit is smaller because of the weaker interaction with the support. Further evidence of the mobility of supported metal oxides on silica has recently been observed by Jehng and Wachs when studying mixtures of vanadia/silica physically mixed with titania (25). Upon calcination, all the surface vanadia migrated from the silica to the titania support due to the greater affinity of titania for surface vanadia. In a similar way, the presence of basic cations, like Na, with higher affinity for the surface molybdenum oxide species than the silica support will act as nucleation centers for these species so relatively low sodium levels will aggregate relatively large amounts of molybdenum oxide. At low sodium contents, some two-dimensional compounds will be formed, probably without well-defined structures, and at higher sodium contents well-defined crystalline structures will be formed (8).

4.2. Catalytic Activity

The effect of sodium on the methane oxidation activity is dramatic, even in those samples where its low loading does not result in significant changes in the Raman spectrum. Concentrations of sodium as low as 300 wppm decrease the catalytic activity for oxidation of methane and methanol to half that of the almost sodium-free sample (10 wppm Na). Methane activation takes place at high temperatures which results in methyl radicals that can react with the supported molybdenum oxide species to generate formaldehyde (5, 26). The pronounced effect of sodium on the Mo/SiO_2 catalysts is due to the strong nucleation effect of sodium which forms new alkali-molybdate clusters and compounds. The amount of the remaining isolated surface molybdenum oxide species has been estimated from the intensity of the Raman band at ca. 986 cm^{-1} (normalized to the Raman band of the silica support at ca. 495 cm^{-1} which can be considered as constant). From the similar behavior of the formaldehyde T.O.F. and the amount of remaining isolated surface molybdenum species as a function of Na loading (Fig. 7a), it appears that the isolated surface molybdenum oxide species are more active than the sodium molybdate cluster/compounds for the selective conversion of the methyl radicals to HCHO. Thus, the addition of sodium appears to eliminate the dispersed surface molybdenum oxide species. Consequently, the T.O.F.s to formaldehyde may be calculated on the basis of the remaining surface molybdenum oxide species and is presented in Fig. 7b. The

T.O.F. values obtained for methane oxidation to formaldehyde become fairly constant with the exception of the sample with the highest sodium loading. It seems, therefore, that the poisoning mechanism involves the interaction of each sodium atom with several individual surface molybdenum oxide species and not with a two-dimensional crystalline lattice which was previously postulated (11). The significant deviation observed in the sample with the highest sodium loading may be a consequence of the presence of new Raman bands in the wavenumber region close to the vibrational mode of the terminal Mo = O bond which makes the quantification of the band at 986 cm^{-1} somewhat difficult.

The effect of sodium on the methanol oxidation reaction is shown in Fig. 8. The presence of sodium also has a negative effect on the methanol oxidation activity which decreases to half of its initial value by the addition of amounts of sodium as low as 300 wppm. Surprisingly, further increases in the amounts of sodium do not show a clear effect on the activity. It is clear that these two reactions follow different mechanisms since the presence of sodium affects methanol and methane selective oxidation to formaldehyde in somewhat different ways. In the oxidation of methanol the molecule first adsorbs dissociatively on the molybdenum site, resulting in the formation of adsorbed CH_3O. These surface methoxy intermediates are easily formed on supported (27, 28) and unsupported (29, 30) metal oxides. The further abstraction of a hydrogen atom by an adjacent oxygen atom results in the formation of adsorbed HCHO which subsequently desorbs as gaseous formaldehyde. Thus, the oxidation of methanol proceeds via oxidative dehydrogenation steps ($CH_3OH \rightarrow CH_3O_{ads} \rightarrow HCHO_{ads} \rightarrow HCHO$) and oxygen insertion into the reactant molecule is not involved. However, methanol oxidation requires a reactive oxygen to be present in order to remove the hydrogen atoms from O–H and C–H bonds. Any modification of this ability results in changes in catalytic activity for the selective oxidation of methanol since isotopic studies have shown that breaking the C–H bond is the rate determining step in this reaction (31, 32). The activity of the oxygen or the amount of reactive oxygen in a catalyst can be measured from the amount of hydrogen consumed in TPR experiments. The parallel trends between the H_2 consumption and the methanol T.O.F. (see Fig. 8) suggest that the capacity of the catalyst to react with hydrogen is the determining factor in the selective oxidation of methanol on silica-supported molybdenum oxide catalysts, and that alkali cations decrease the amount of available reactive oxygen by the formation of new alkali–molybdate compounds.

All the alkali-metal-doped samples show reduced activity for methane and methanol oxidation compared to the pure molybdena/silica catalysts (Table 1), but the trends in poisoning are rather different for these two reactions.
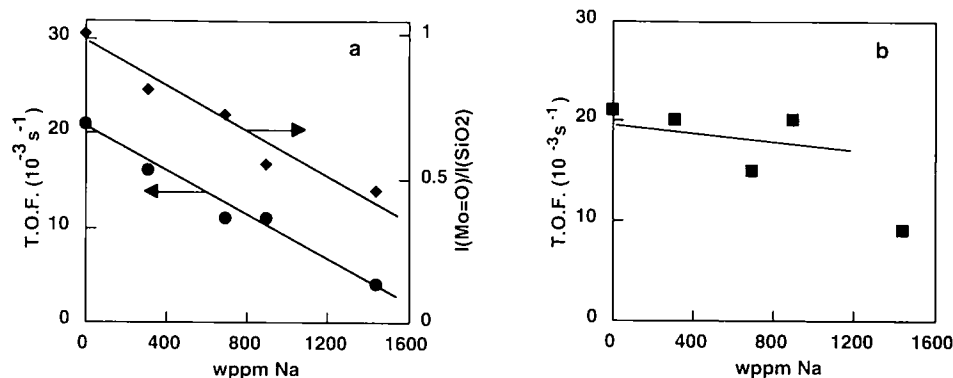
FIG. 7. (a) Comparison of the formaldehyde T.O.F. from CHy and the amount of dispersed surface molybdenum oxide species. (b) Formaldehyde T.O.F. from CHy referred to the amount of remaining dispersed surface molybdenum oxide species as a function of the sodium loading. Reaction conditions are explained in Table 1.

For methane oxidation the degree of poisoning is Na $\gg$ Cs > K, and for methanol oxidation the order is K > Cs > Na. The most affected products in methane oxidation are HCHO and CO, and their T.O.F.s show a profound decrease. Meanwhile, CO_2 shows a minimum variation in the Cs-doped sample and a significant increase in the K-doped sample. However, during methanol oxidation the most affected product is formaldehyde which decreases about a factor of three in the sequence Na, Cs, K. However, the tendency of hydrogen uptake reported in Table 1 is not reflected in the oxidation of methanol.

5. CONCLUSIONS

1. The surface molybdenum oxide species readily interact with alkali metals to form new alkali–molybdate compounds because of their weak interaction with the silica

FIG. 8. Comparison of methanol T.O.F. and hydrogen comsumption during the TPR experiments. Reaction conditions are explained in Table 1.

support and the strong acid–base interactions between the alkali and molybdenum oxide components. Consequently, the number of isolated surface molybdenum oxide species on silica decreases with increasing alkali loading.

2. The addition of alkali to the silica-supported molybdenum oxide catalysts generally decreases the amount of reducible oxygen available in the catalysts are revealed by temperature programmed reduction studies.

3. The catalytic activity for methanol oxidation over the alkali-doped molybdena/silica catalysts was generally found to correlate with the amount of reducible oxygen in the catalyst as well as the alkali type and loading.

4. The surface molybdenum oxide species are fully oxidized under methane oxidation conditions and possess the same structure as that found under dehydrated conditions.

5. The catalytic activity for methane oxidation over the alkali-doped molybdena/silica catalysts was found to correlate with the number of isolated surface molybdenum oxide species present on the silica support. This suggests that the isolated surface molybdenum oxide species are the active sites for methane oxidation.

6. The somewhat different responses of the methane oxidation and methanol oxidation reactions over the Mo/silica catalysts to the alkali poisoning reflects their different reaction mechanisms (oxygen insertion/dehydrogenation and oxidative dehydrogenation, respectively) of those two different reactions producing formaldehyde.
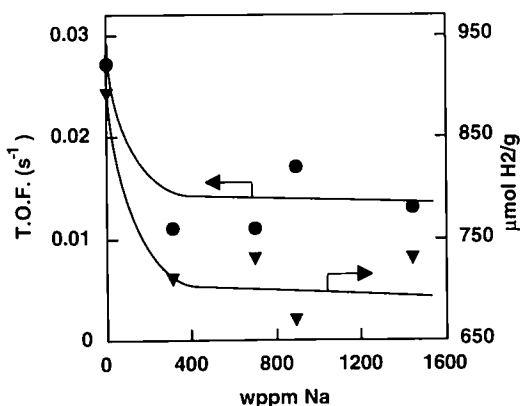
REFERENCES

1. Spencer, N. D., and Pereira, C. J., *J. Catal.* **116**, 399 (1989).
2. Yang, T. J., and Lunsford, J. H., *J. Catal.* **103**, 55 (1987).
3. Moffat, J. B., and Kasztelan, S., *J. Catal.* **109**, 206 (1988).
4. Weng, T., and Wolf, E. E., *in* "Symp. Natural Gas Upgrading II, ACS, April, 5–10, 1992," p. 46.
5. Sun, Q., Di Cosimo, J. I., Herman, R. G., Klier, K., and Bashin, M. M., *Catal. Lett.* **15**, 371(1992).
6. Burch, R., and Baldwin, T. D., *Appl. Catal.* **74**, 137 (1991).
7. Bañares, M. A., and Fierro, J. L. G., *Catal. Lett.* **17**, 205 (1993).
8. Williams, C. C., Eckerdt, J. G., Jehng, J. M., Hardcastle, F. D., Turek, A. M., and Wachs, I. E., *J. Phys. Chem.* **95**, 8781(1991).
9. de Boer, M., van Dillen, A. J., Konigsberger, D. C., Geus, J. W., Vuurman, M. A., and Wachs, I. E., *Catal. Lett.* **11**, 227(1991).
10. Spencer, N. D., *J. Catal.* **109**, 187(1988).
11. Spencer, N. D., Pereira, C. J., and Grasselli, R. K., *J. Catal.* **126**, 546(1990).
12. Spencer, N. D., and Pereira, C. J., *AIChE J.* **33**, 1808(1987).
13. Deo, G., and Wachs, I. E., *J. Catal.* **129**, 307 (1991).
14. Hardcastle, F. D., and Wachs, I. E., *J. Raman Spectrosc.* **21**, 683 (1990).
15. Becher, Von H. J., *Z. Anorg. Allg. Chem.* **474**, 63 (1981).
16. Bañares, M. A., Rodríguez-Ramos, I., Guerrero-Ruíz, A., and Fierro, J. L. G., *in* "Proceedings, 10th International Congress on Catalysis" (L. Guczi, Ed.) p. 1131. Akademia Kiadó, Budapest 1993.
17. Koranne, M. M.; Goodwin Jr., J. G. and Marcelin, G., *in* "Symp. on Natural Gas Upgrading II, ACS, April, 5–10, 1992, p. 41.
18. Mauti, R. and Mims, C. A., *in* "Symp. on Natural Gas Upgrading, ACS, April, 5–10, 1992," p. 65.
19. Vuurman, M. A., and Wachs, I. E., unpublished results.
20. C. C. Williams, "Synthesis, Characterization and Reactivity of Oxide Supported Molybdenum Oxide." Ph.D. Thesis, The University of Texas at Austin, 1990.
21. Leyrer, J., Mey, D., and Knözinger, H., *J. Catal.* **124**, 349(1990).
22. Martín, C., Mendizabal, M. C., and Rives, V., *J. Mater. Sci.* **27**, 5575 (1992).
23. Stampfl, S. R., Chen, Y., Dumesic, J. A., Chunming, N., and Hill, C. G., *J. Catal.* **105**, 445 (1987).
24. Wachs, I. E., Deo, G., Vuurman, M. A., Hu, H., Kim, D. S., and Jehng, J. M., *in* "Proceedings, 10th International Congress on Catalysis" (L. Guczi, Ed.), p. 543. Akademia Kiadó, Budapest, 1993.
25. Jehng, J.-M., and Wachs, I. E., unpublished results.
26. Tong, Y., and Lunsford, J. H., *J. Am. Chem. Soc.* **113**, 4741 (1991).
27. Kim, D. S., Ph.D. Thesis, Sophia University, Tokyo, 1990.
28. Busca, G., *J. Mol. Catal.* **50**, 241 (1989).
29. Morrow, B. A., *J. Chem. Soc Faraday Trans 1* **70**, 1527 (1974).
30. Busca G., and Loenzelli, V., *J. Catal.* **66**, 155 (1980).
31. Yang, T. J., and Lunsford, J. H., *J. Catal.* **103**, 55 (1987).
32. Machiels, C. J., and Sleight, A. W., *J. Catal.* **76**, 238 (1982).